Tensile stress development and critical behavior of a flexible barrier

Miao Huo[1*] , *Fucheng* Huang[1], *Maojun* Yang[1], and *Chenjie* Jiang[1]

[1]College of Water Conservancy and Hydropower Engineering, Sichuan Agricultural University, Ya'an city 625014, China

Abstract. A DEM numerical approach is employed to illustrate the critical stress development of a three-supporting cable flexible barrier under a large scale stony debris movement impact. A proper linear parallel bond is applied to build the flexible barrier model. Critical state is presented by lowering the tensile resistance of the flexible barrier and steepening the channel slope. The tensile stress of the supporting cables is primarily studied. Results mainly indicate that the particle-structure contact is essential to the stress development. The bottom cable always exhibits larger tensile stress due to the massive collision and compressive force of particles and the tensile force exerted by the vertical cable-net joint system. On the other hand, the intermediate cable receives lower collision and compressive force, resulting in smaller tensile stress. The bottom cable indicating numerous direct particle-structure contact part performs brittle failure, which is analogous to the concentrated load feedbacks. The loading of the intermediate one reaches ductile failure, reflecting the desirable effect of dispersing loads. This study suggests that practical engineering should try to avoid massive boulder impact or reinforce the bottom cable in order to improve the hazard prevention design.

1 Introduction

The flexible barrier shows its broad prospect in preventing mountainous hazards such as rock avalanche, landslide and debris flow. The critical state of flexible barrier is key to verify the reliability. Increasing research works have been taking the structural failure into account. Albaba [1] analyzed load transfering process of the supporting cable under the action of debris flow particles by DEM numerical simulation and revealed that the stress of the anchor foundation was related to the installation site, the energy dissipator and the interception. CFD-DEM has been adopted to simulate the flexible barrier without supporting cable bearing the debris-flow impact and it indicates the breakage at middle section and end of the bottom net is the commerce of failure [2]. Albrecht and Volkwein [3] studied the dynamic response of a flexible barrier with rhombic net structure subjected to boulder-impact, and the failure characteristics of the structure under concentrated load are described.

Previous studies have paved a solid way for the critical state verification of flexible barrier. This study aims to perform a rapid numerical analysis on flexible barrier under critical debris-flow impact and to estimate the stress development from initiated to final process.

2 Methodology

Collision of particles without fluid on the flexible barrier is mainly studied through Particle Flow Code in three dimension i. e. PFC^{3D}, due to the dominate role of solid fraction in the impact mechanism [4]. The impact scenario is demonstrated by a total solid volume of 400 m^3 (apparent volume) accelerating along a inclined chute and hitting the flexible barrier at the end of the chute (Fig. 1 and Table 1). Here we employ the particle-particle parallel bond (abbreviated as p. b.) to build the cable-net structure and set the net before the cables to ensure the transferal force on the cables. Constrainted particle size distribution is introduced (Table 2), constituting a stony debris flow, and energy dissipator component is not planted, for simplified calculation. Three identical-spacing cabes are employed to support the net structure (Table 2) due to the elusive postion of one cable that uniformly bears the distributed impact load, and the mesh size of the net is equal to the maximum grain size of the debris material based on an open-type dam [5]. The theory of the bond technology can be reviewed in the literature [6]. The initiation of the debris particle is a dam-break technique and then produces a laminar flow through the rectangle-section chute to impact the flexible barrier model. The stress of one cable can be monitored by the p. b.-stress module which is invoked in the software. The tensile strength of the cable is lower than the actual yield strength in order

* Corresponding author: huomiao@sicau.edu.cn

to meet the critical state efficiently (Table 2). Moreover, we use a conventional expression of safety factor K to depict the structural behavior, especially the critical state as follow.

$$K = \frac{\sigma_{pb}}{\sigma_t} \quad (1)$$

Where σ_{pb} and σ_t are the tensile resistance of p.b. (500 MPa) and detected normal tensile stress, respectively.

Table 1 Dimension of the chute

Length (km)	Width (m)	Slope	Cross-section (m)	Total initiation volume (m^3)
0.025	16	45°	16×16	400

Table 2 Dimension of flexible barrier and debris flow

Objective	Density (kg/m^3)	Diameter of cable/maximum grain (mm)	Diameter of net/minimum grain (mm)	Cable spacing (m)	Mesh size (m)
Flexible barrier	5300	32	10	4	1.6
Debris particles	2500	1600	30	-	-

3 Results

The calculation duration is short and the total compute time of this simulation is around 3 hours. Right before the impact, the debris particle flow is around 3.4 m in mean thickness and 1.5 m per second in mean velocity, forming an impact energy of approximately 810 kJ. Then the particle interception rate (in weight) of the structure is 69.14%.

The factor K of every p. b. node in the structure is displayed in Fig. 2, and major part of the top, immediate and bottom cable, including the net structure is in critical state but some part of the net is still in stable i. e. very great value of K. Furthermore, large-particle collision with the bottom cable is notable, leading initial tensile damage at the left lateral point of the bottom cable. Breakage practically extends from bottom to the immediate as the impact processing.

The tensile stress of the bottom cable is always greater than that of the intermediate cable. The stress increment and the rupture of bottom cable are sharp and instant, respectively, while it takes a long time span (around 8 seconds) for the immediate cable to reach the failure state (Fig. 3).

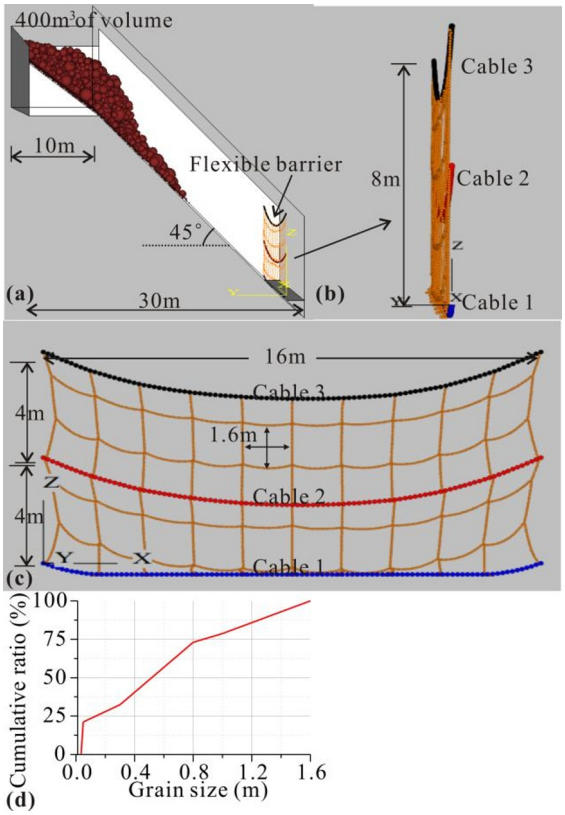

Fig. 1. Diagram of numerical simulation: (a) profile of overall impact scene (b) cross-section of the flexible barrier model (c) the elevation view of the flexible barrier from downstream site and (d) grain distribution of the debris material.

4 Conclusion and implication

The critical state mainly stems from the bottom cable that receives massive particle-collision, earth pressure and the tensile force exerted by the vertical cable-net joint system, and subsequently extends to global structure as the impact loading, ending up to overall failure. Stress developments indicate that the bottom cable performs brittle-like rupture, while the intermediate reaches ductile failure and reflects the desirable effect of dispersing loads. In practice, the lateral part of the bottom cable, enduring the sum of impact load along the cable, deserves mechanical care or reinforcement. As one kind of tension structures, the flexible barrier subjected to debris particle impact would perform evident geometric nonlinearity. This numerical simulation limits the yield strength of the cable, which seems not rigorous in the similarity theorem. But the loading developments (of strength limitation or not) before failure share the same trend, and this numerical framework enables us to analyze the load response and failure rapidly. What's more, only several parameters and dimensions would be retyped to study other relevant engineering cases.

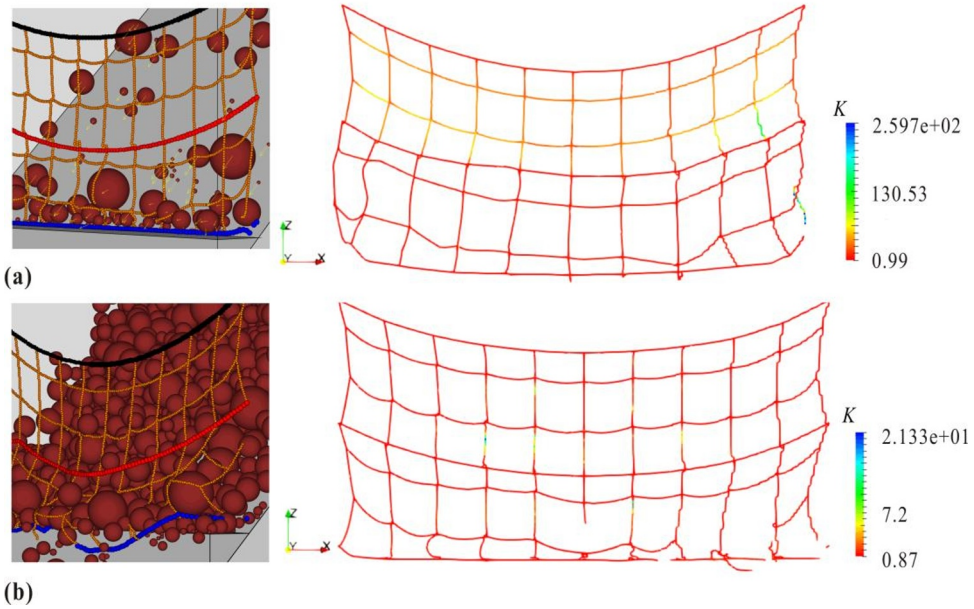

Fig. 2. The safety factor *K* distributed in the structure: (a) the initial impact stage and (b) the later impact stage of the critical impact.

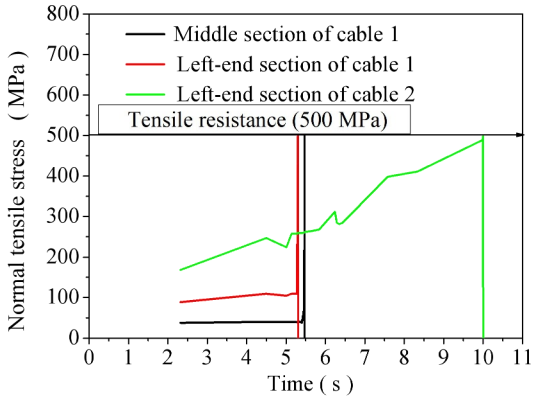

Fig. 3. Tensile stress development of the cables.

References

1. A. Albaba, Univ. Grenoble Alpes (2015)
2. X. Y. Li, J.D. Zhao, Int. J. Numer. Anal. Meth. Geomech., **42**, 14, 1643 (2018)
3. V. B. Albrecht, A. Volkwein, Can. Geotech. J., **56**, 3, 398 (2019)
4. S. He, W. Liu, X. Li, Environ Earth Sci., **75**, 4, 298 (2016)
5. T . Mizuyama. Int. J. E. C. E., **1**,2, 38 (2008)
6. R. Jiang, W. P. Fei, H. W. Zhou, M. Huo, J. W. Zhou, J. M. Wang, J. J. Wu, B. Eng. Geol. Environ. **79**, 2213 (2020)